Effects of compressive epitaxial strain on the magnetotransport properties of single-phase electron-doped La 0.7 Ce 0.3 MnO 3 films

W. J. Chang, C. C. Hsieh, J. Y. Juang, K. H. Wu, T. M. Uen, Y. S. Gou, C. H. Hsu, and J.-Y. Lin

Citation: Journal of Applied Physics **96**, 4357 (2004); doi: 10.1063/1.1792808
View online: http://dx.doi.org/10.1063/1.1792808
View Table of Contents: http://scitation.aip.org/content/aip/journal/jap/96/8?ver=pdfcov
Published by the AIP Publishing

Effects of compressive epitaxial strain on the magnetotransport properties of single-phase electron-doped $La_{0.7}Ce_{0.3}MnO_3$ films

W. J. Chang, C. C. Hsieh, J. Y. Juang, K. H. Wu, T. M. Uen, and Y. S. Gou
Department of Electrophysics, National Chiao Tung University, Hsichu, Taiwan

C. H. Hsu
National Synchrotron Radiation Research Center, Hsinchu, Taiwan

J.-Y. Lin
Institute of Physics, National Chiao Tung University, Hsinchu, Taiwan

(Received 16 April 2004; accepted 25 July 2004)

Single-phase electron-doped manganite thin films with nominal composition of $La_{0.7}Ce_{0.3}MnO_3$ (LCeMO) have been prepared on $SrTiO_3$ (100) substrates by pulsed laser deposition. The conditions for obtaining purely single-phase LCeMO films lie within a very narrow window of substrate temperature ($T_s \sim 720$ °C) and laser energy density ($E_D \sim 2$ J/cm^2) during deposition. *In situ* postdeposition annealing, mainly to relax the possible epitaxial in-plane tensile strain between the film and the substrate, leads to an increasing c-axis lattice constant accompanied by the formation of secondary CeO_2 phase and higher metal-insulator transition temperature. This is indicative of a strong coupling between the electron and lattice degree of freedom. © *2004 American Institute of Physics*. [DOI: 10.1063/1.1792808]

I. INTRODUCTION

Owing to the colossal magnetoresistance (CMR) for the practical application potential in the so-called "spintronics" and the rich phase diagrams arising from competing order parameters, the hole-doped manganites, in the forms of $R_{1-x}A_xMnO_3$ (R, rare-earth ion; A, divalent cation), have been attracting a rapt attention over the last decade or so. One of the most salient features exhibited by this class of materials is the paramagnetic-ferromagnetic transition accompanied by an insulating to metallic transition (MIT) at nearly the same temperatures characterized as Curie temperature (T_C) and insulator-metal transition temperature (T_{IM}), respectively. The origin of these effects, after tremendous evidences cumulated from both theoretical and experimental studies, appears to be well beyond the framework of the ubiquitously adopted double-exchange (DE) mechanism,[1,2] in that the hopping of e_g^1 electron between Mn^{3+} and Mn^{4+} is the only significant prevailing process. For instance, the large resistivity value above T_C (Ref. 3) and the nanoscale phase separation in nominally homogeneous samples[4,5] cannot be comprehended by the DE mechanism.

On the other hand, it has been widely anticipated that electron-doped $RMnO_3$ compounds obtainable by replacing the divalent dopants with tetravalent ones (e.g., cerium or tin) should also possess similar CMR effects.[6–10] The intuitive argument for this direct analogy is that Mn^{2+} and Mn^{4+} are non-Jahn-Teller ions and the hopping of e_g^2 electron between spin-aligned Mn^{2+} and Mn^{3+} should be similar to that between Mn^{3+} and Mn^{4+}. Earlier studies[6–10] of these electron-doped manganites indeed reproduced most of the electric and magnetic properties of their hole-doped counterparts; e.g., $La_{0.7}Ce_{0.3}MnO_3$ (LCeMO) displayed similar temperature dependent resistivity $[R(T)]$ and magnetization $[M(T)]$ behaviors with almost the same T_{IM} and T_C as that of the hole-doped $La_{0.7}Ca_{0.3}MnO_3$ (LCMO). Based on the consideration of ion size constraints, however, Joseph Joly, Joy, and Date[11] have argued that it is generally impossible to substitute the trivalent La^{3+} with a tetravalent ion, such as Ce^{4+} and Sn^{4+} via conventional solid-state reaction processes. They further questioned that the single-phase polycrystalline and expitaxial LCeMO films reported by Mitra *et al.*[8] might have been the self-doped $La_{1-x}MnO_{3-\delta}$ manganites.[12,13] The issues, nevertheless, have been pretty much settled by a series of papers published by Mitra *et al.*,[14–16] wherein direct observation of electron doping in LCeMO by x-ray absorption spectroscopy (XAS),[14] the current-voltage characteristics from LCeMO/LCMO *p-n* junctions,[15] and LCeMO/STO/LCMO tunnel junctions[16] all evidencing that LCeMO is indeed an electron-doped manganite.

Despite these remarkable progresses in this relatively new material, there are some issues that remain to be clarified. For instance, Mitra *et al.*[8] argued that it is desirable to use high laser energy density ($E_D \sim 3$ J/cm^2) and high T_s(>750 °C) to obtain single-phase LCeMO films. This is somewhat mysterious considering that both factors are in favor of forming the more stable CeO_2. In addition, it is also suggested that the double-peak MIT transition frequently observed in mixed-phase LCeMO bulks is mainly due to the presence of the unreacted CeO_2. In this study, we perform a detailed study on the formation of LCeMO phase by systematically varying the T_s, E_D, as well as the duration of *in situ* annealing carried out immediately after deposition. The results clearly demonstrate that single-phase LCeMO films can only be obtained at much lower T_s (~720 °C as compared to >750 °C) with a smaller E_D (~2 J/cm^2 as compared to 3 J/cm^2).[17] Furthermore, we note that, while the *in situ* postdepositon annealing has inevitably induced the formation of CeO_2 phase, it also raises T_C and T_M with apparent c-axis

lattice parameter relaxation towards the bulk value. The compressive strain originated from the epitaxial relation $a_{STO} > a_{LCeMO}$ and the associated suppression in T_{IM} and T_C suggested the prominent coupling between the electron and lattice degree of freedom in CMR effect.

II. EXPERIMENT

Target with nominal composition of $La_{0.7}Ce_{0.3}MnO_3$ was prepared by mixing stoichiometric amount of CeO_2, La_2O_3 (which had been preheated), and $MnCO_3$ powders in a mortar. The mixture was heated in air at 1100 °C for 20 h. The agglomerated substance was then ground, palletized, and sintered at 1400 °C for 27 h. The last step was repeated once to maximize reactions between the ingredients. The target thus obtained was a mixed-phase material and exhibited a broad double-peak MIT transition at 200 and 240 K, respectively. These characteristic properties are similar to that of the typical polycrystalline bulks reported previously.[18] Epitaxial LCeMO films were grown on STO substrate by pulsed laser deposition, using a KrF (248 nm) excimer laser with a repetition rate of 5 Hz. We first scan deposition parameters such as oxygen pressure, T_s and E_D to give a rough optimization on T_C and T_{IM} of the films. For this study, while other parameters were varied for investigating the issues mentioned above, an oxygen pressure of 0.35 Torr was set for all experiments as it gave the best results. Moreover, in order to delineate possible strain effects, the films thickness was kept at 100 nm for all the films used in this study. For *in situ* annealing (see below), the chamber was filled with pure oxygen to about 500 Torr immediately after deposition while keeping the substrate temperature at 720 °C for various periods of time before cooling to room temperature. As revealed by x-ray diffraction (XRD), all the films display well-oriented characteristic with c-axis normal to film plane. In order to check the film/substrate epitaxial relation, we also performed the reciprocal lattice scattering with synchrotron radiation x-ray and in-plane ϕ-scan experiments. The results clearly indicate the highly epitaxial characteristic between the films and the substrate. The transport $[R(T)]$ and magnetization $[M(T)]$ properties as functions of temperature and applied field were carried out in a Quantum Design® PPMS system.

III. RESULTS AND DISCUSSION

Figure 1 shows a summary of XRD results demonstrating how the formation of single-phase LCeMO and accompanying CeO_2 phases were dependent on T_s, E_D, and *in situ* annealing. The deposition and treatment conditions of the LCeMO films together with the crystalline parameters were collected in Table I. The enlarged XRD trace shown in the upper right inset of Fig. 1 shows the high c-axis oriented characteristic of the films. It is also evident from Fig. 1 that single-phase LCeMO can only be obtained within a very narrow window around $T_s \sim 720$ °C with $E_D = 2$ J/cm^2. Merely raising or lowering T_s by 10 °C or increasing E_D to 3 J/cm^2 leads to the formation of CeO_2 phase. These results show some disagreements with the conjecture reported by Mitra *et al.*,[8] where high laser energy density and high T_s

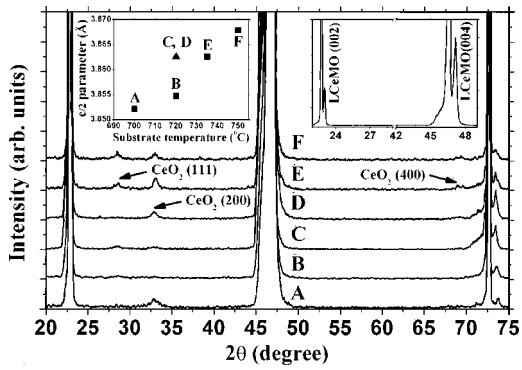

FIG. 1. XRD results of sample A to F. Notice trace amount of CeO_2 phase can be identified in all cases, except for B. The upper-left inset denotes the variation of c-axis lattice constant with the relaxation of in-plane tensile strain induced by the increase of T_s, annealing (sample C), and high E_D deposition (sample D). The upper-right inset shows excellent epitaxial relation between LCeMO (002) and STO substrate.

were considered to be desirable for obtaining single-phase LCeMO films. Although, the discrepancy may be simply due to the systems used. However, since there is a clear tendency of expanding c-axis parameter with increasing T_s (see the upper left inset of Fig. 1 and the last column of Table I) we argue that the strain state of the growing film might have played a very important role. To further delineate the argument, the film/substrate epitaxial relation has been carefully checked with more delicate synchrotron x-ray scattering as well as ϕ-scan measurements.

As shown in Fig. 2, x-ray scattering results show that the deposited LCeMO indeed forms a high quality epitaxial film on the STO substrate. The dash and solid lines in Fig. 2(a) depict the distribution of scattered x-ray intensity along (001) direction (l-scan) in the neighborhood of (002) and (112) Bragg peaks. The stronger peaks centered at $l=2$ rlu (reciprocal lattice unit) are originated form the STO substrate and the weaker peaks centered at 2.016 rlu are coming from the LCeMO epitaxial film. The larger l value of the film peaks reveals that its lattice constant along the c axis is 0.8% shorter than that of the substrate. The difference, though is slightly smaller than that estimated from the XRD results for sample B ($\sim$1.2%) using the bulk lattice constants of the relevant phase involved here, namely, $a=3.902$ Å for STO, $a=5.403$ Å, $b=5.518$ Å, $c=7.759$ Å for bulk LCeMO.[18] It is, nevertheless, much larger than the difference of about 0.58% between $(c/2)_{LCeMO}$ and c_{STO} expected with the absence of epitaxy-induced compressive strain along the c axis.

The in-plane crystallographic orientation of the film with

TABLE I. Summary of deposition conditions for the representative films studied. All films were deposited at fixed $PO_2 = 0.35$ Torr.

Sample	T_s(°C)	E_D(J/cm^2)	Postannealing	$c/2$ parameter (Å)
A	700	2	No	3.852
B	720	2	No	3.855
C	720	2	60 min	3.863
D	720	3	No	3.863
E	735	2	No	3.863
F	750	2	No	3.868

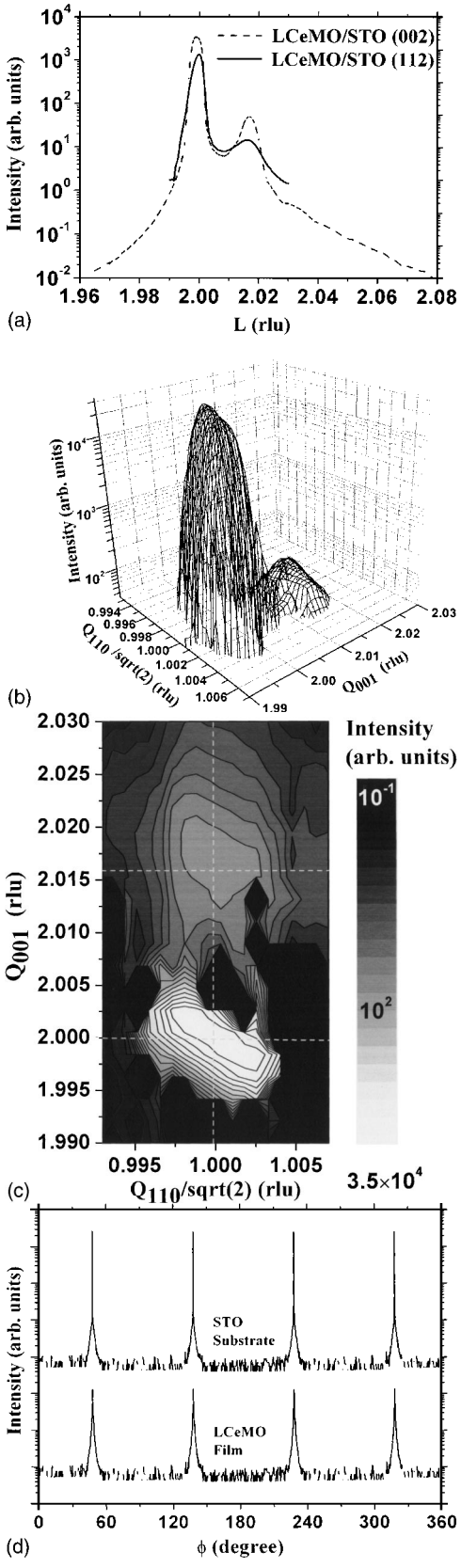

FIG. 2. (a) X-ray intensity distribution along the (001) direction of both (002) and off-specular (112) Bragg peaks. (b) The 3D distribution of the scattered x-ray intensity on the [110] plane near the (112) Bragg peaks. (c) The contour plot of the intensity distribution around the (112) Bragg peak. (d) Φ scans around the (001) axis across the (1 1 2.016) peak of the LCeMO film (lower curve), and that across the (112) peak of the substrate (upper curve), showing the excellent in-plane alignment between the film and the substrate.

respect to the substrate was further examined by the intensity map of the off-specular (112) Bragg peaks and the ϕ-scan measurements around (001) axis across the (1 1 2.016) peak. As shown in Fig. 2(b), in addition to the strong substrate peak centered at (112), a weak bump centered at (1 1 2.016) rlu, which is associated with the (112) Bragg peak of the LCeMO film was clearly observed. Figure 2(c) shows the contour mapping of the scattering intensity and displays essentially the same features. Furthermore, the ϕ-scan measurements around (001) axis across the substrate (112) and film (1 1 2.016) peaks are displayed in Fig. 2(d) for comparison. It is clear that both ϕ scans show four distinct peaks lining up with each other. All this information confirmed that the lattice of the LCeMO film is in good registry with that of the STO substrate and their in-plane axes are aligned with each other. These independent measurements thus lend strong support to the conjecture that the epitaxy-induced strain and its effects on the film c-axis parameter are indeed very sensitive to deposition and treatment conditions.

It is also interesting to note that for films grown at higher T_s both (111) and (200) orientations of CeO_2 are present, while only (200) orientation appears in films deposited at $T_s = 700\ ^\circ C$. It turns out that by rotating the *a*-*b* plane of both LCeMO and CeO_2, they can actually get quite good lattice matching with STO substrate. Early developments of biepitaxial high-T_c superconducting grain boundary junctions using CeO_2 as the buffer layer to provide a 45° rotation[19] and the TiO_2-buffered biepitaxial $La_{0.7}Ca_{0.3}MnO_3$ step junctions[20] have all utilized exactly this effect. This rotation, though gives good epitaxial relations between the relevant phases, still results in a slight in-plane tensile stress to the films. At higher T_s and/or after prolonged annealing, the accumulated strain starts to relax by generating dislocation-related extended defects or by forming the secondary CeO_2 phase, leading to the relief of in-plane tensile stress. As the in-plane tensile stress is relaxed, the c-axis lattice constant of LCeMO films approaches toward its bulk value. Similarly, films prepared with $E_D = 3\ J/cm^2$ (trace D) and that subjected to long time annealing (trace C) behave well along the expected trend. Moreover, the fact that CeO_2 phase does not appear in every case indicates that it may not form directly from the target residues.[8] Rather, the formation of CeO_2 should be a direct consequence of strain relaxation, which could occur during deposition or be promoted by annealing afterward. At low enough T_s, CeO_2 maintains epitaxial relation with STO substrate and is formed preferably along (100) orientation. While at higher temperatures the substrate effect is diminished, leading to a structure with randomized grain orientation, as seen in traces E and F of Fig. 1.

Having disclosed the detailed crystalline structure for films grown under various conditions, we turn to discuss how the strain state affects the electric and magnetic properties of the LCeMO. Figure 3(a) shows the $R(T)$ results of the as-deposited film (B) and films annealed at 720 °C and 500 Torr of oxygen for 10, 30, and 60 min (C), respectively. We note that for this series of films only the C film shows trace of CeO_2 phase in XRD (trace C in Fig. 1). As is evident from the $R(T)$ curves, there is only one MIT transition in each sample and T_{IM} is progressively improved from 255.5

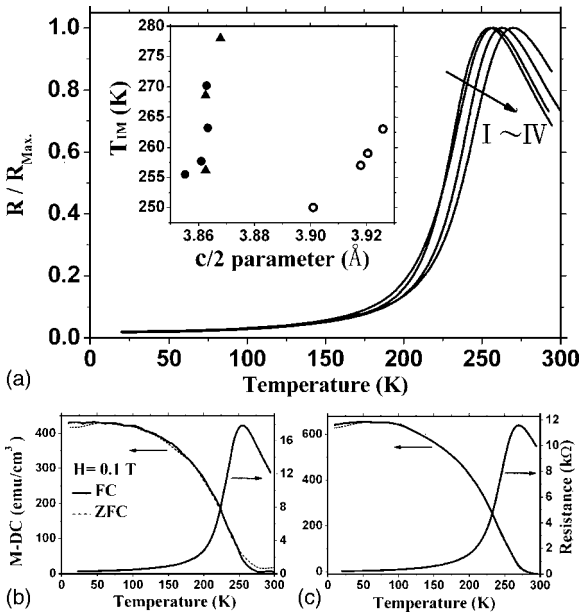

FIG. 3. (a) Effect of *in situ* annealing on the MIT behavior of single-phase LCeMO films. T_{IM}'s are 255.5, 255.7, 263.2, and 270.2 K for films annealed by 0, 10, 30, and 60 min (denoted in order from I to IV), respectively. The inset illustrates the relaxation of tensile in-plane strain induced by annealing (solid circles) and higher T_s (solid triangles) can lead to c-parameter expansion with enhanced T_{IM}. Open symbols are taken from Ref. 17 for comparing the effect of compressive in-plane strain on T_{IM}. (b), (c) $R(T)$ and $M(T)$ curves of sample B and sample C, respectively. Notice that there are no apparent hystereses between field-cooled and zero-field-cooled $M(T)$'s.

to 270.2 K with increasing annealing time. We believe that the latter should be the more significant one. Haghiri-Gosnet *et al.*[21] reported how the tensile and compressive strains alter the easy magnetization orientation in $La_{0.7}Sr_{0.3}MnO_3$ films. Though they did not make detailed comparison of the effect on T_{IM}, the deviation of Mn-O bond angle from its normal configuration and, hence, the CMR properties can be expected, at least qualitatively. To this end, we further analyzed how the change of c-axis lattice constant affects T_{IM}. The results are shown as the solid circles in the inset of Fig. 3(a). The relaxation of the in-plane tensile strain (reflected by increasing *c* parameter) evidently enhances T_{IM}. Shown also in the inset of Fig. 3(a) are the results from films deposited at different T_s's (solid triangles) and that taken from Ref. 7 (open circles) for LCeMO films deposited on $LaAlO_3$ substrates which gives in-plane compressive strain on the films. The relaxation of strain in Ref. 7 was obtained by increasing the film thickness, thus might not be complete. Although the absolute T_{IM} is apparently system dependent and there might still be some subtle calibrations needed to get the *c* parameters derived form both experiments in order, it nevertheless, indicates a generic tendency of how strain state affects the CMR properties of the electron-doped LCeMO manganites. It appears that in-plane tensile strain tends to deteriorate T_{IM} while the compressive strain does the opposite. This is indicative of a strong coupling between the electron and the lattice degree of freedom existent in this system.

Finally, $R(T)$ and $M(T)$ with that of films B and C are illustrated in Figs. 3(a), 3(b), and 3(c). It is clear that unlike those found in bulk LCeMO, there is no sign of double transition in $R(T)$ curves in all cases. In addition, except for the slight differences in T_{IM} (255 and 270 K for B and C, respectively), the presence of CeO_2 in the films does not seem to result in any noticeable influence on the $R(T)$ transitions. Although this is in contrast to the speculation of attributing the double transition to the existence of CeO_2 originally proposed by Mitra *et al.*,[8] it might be due to the small amount of CeO_2 existent in our films. Interesting features to be noted are the subtle differences in the $M(T)$ curves. First, the saturation magnetization is about 30%–40% smaller in the as-deposited single-phase LCeMO (B) as compared to that of C, wherein CeO_2 is present. In that, the small shift of $M(T)$ has been attributed to a ferromagnetic spin canting transition commonly observed in poorly oxidized manganites and can be removed by postannealing to increase the Mn^{4+}/Mn^{3+} ratio. It is not clear at present whether similar argument applies to the electron-doped case or not. Alternatively, it is often suggested that prolonged oxygen annealing may result in hole-doped La-deficient ($La_{1-x}MnO_3$) phase with predominate existence of Mn^{3+} and Mn^{4+} ions.[12,13,22] In such cases, though it may partially account for the magnetization enhancement, significant hysteresis between field-cooled and zero-field-cooled $M(T)$ curves have been ubiquitously observed.[23,24] This apparently is not observed in the present study, implying that our annealing scheme does not lead to the formation of La-deficient or oxygen excessive phase. The other issue of relevance is whether or not Ce^{4+} ions really replace the La ions to make it electron doped? Or can the existence of CeO_2 actually change the electronic states and lead to some specific magnetic phase locally, while giving rise to similar metallic characteristics? Recent measurements,[14,25] including ours,[26] by XAS showed characteristics of the existence of Mn^{2+}, and did not reveal any electronic inhomogeneity. However, to further delineate the electronic structure of material, analyses on the valence state of other elements are desired. Detailed studies on oxygen absorption edge and their temperature dependence are underway and will be reported elsewhere.

IV. CONCLUSION

In summary, we have demonstrated that the conditions of growing single-phase electron-doped LCeMO manganite thin films can be very sensitive to both the substrate temperature and laser energy density. In our case, the optimal conditions are $T_s = 720\ ^\circ C$ and $E_D = 2\ J/cm^2$, which are lower than that used by Mitra *et al.*[8] *In situ* annealing on the single-phase LCeMO films at 720 °C and 500 Torr of oxygen progressively enhances T_{IM} from as-deposited 255 to 270 K after 60 min of annealing. This enhancement is accompanied by an increase of c-axis lattice parameter arisen from relaxation of in-plane tensile strain and is indicative of strong correlation between electron and lattice degree of freedom. The success of preparing the single-phase electron-doped manganite should provide good opportunity for analyzing the role of e_g^2 electrons in CMR effect as well as for exploring new device structures by combining with its hole-doped counterparts.

ACKNOWLEDGMENT

This work was supported by the National Science Council of Taiwan under the Grant No. NSC92-2112-M-009-033.

[1]C. Zener, Phys. Rev. **82**, 403 (1951).
[2]P. G. de Gennes, Phys. Rev. **118**, 141 (1960).
[3]A. J. Millis, P. B. Littlewood, B. I. Shraiman, Phys. Rev. Lett. **74**, 5144 (1995).
[4]E. Dagotto, *Nanoscale Phase Separation and Colossal Magnetoresistance* (Springer, Berlin, 2003), and references therein.
[5]S. F. Chen, P .I. Lin, J. Y. Juang, T. M. Uen, K. H. Wu, Y. S. Gou, and J. Y. Lin, Appl. Phys. Lett. **82**, 1242 (2003).
[6]J. Philip and T. R. N. Kutty, J. Phys.: Condens. Matter **11**, 8537 (1999).
[7]P. Raychaudhuri, S. Mukherjee, A. K. Nigam, J. John, U. D. Vaisnav, R. Pinto, and P. Mandal, J. Appl. Phys. **86**, 5718 (1999).
[8]C. Mitra, P. Raychaudhuri, J. John, S. K. Dhar, A. K. Nigam, and R. Pinto, J. Appl. Phys. **89**, 524 (2001).
[9]Z. W. Li, A. H. Morrish, and J . Z. Jiang, Phys. Rev. B **60**, 10284 (1999).
[10]X. Guo, S. Dai, Y. Zhou, G. Yang, and Z. Chen, Appl. Phys. Lett. **75**, 3378 (1999).
[11]V. L. Joseph Joly, P. A. Joy, and S. K. Date, J. Magn. Magn. Mater. **247**, 316 (2002).
[12]S. Pignard, H. Vincent, J. P. Senateur, K. Flohlich, and J. Souc, Appl. Phys. Lett. **73**, 999 (1998).
[13]S. S. Manoharan, D. Kumar, M. S. Hedge, K. M. Satyalakshmi, V. Prasad, and S. V. Subramanyam, J. Solid State Chem. **117**, 420 (1995).
[14]C. Mitra *et al.*, Phys. Rev. B **67**, 092404 (2003).
[15]C. Mitra, P. Raychaudhuri, G. Köbernik, K. Dörr, K.-H. Müller, L. Schultz, and R. Pinto, Appl. Phys. Lett. **79**, 2408 (2001).
[16]C. Mitra, P. Raychaudhuri, K. Dörr, K. -H. Müller, L. Schultz, P. M. Oppeneer, and S. Wirth, Phys. Rev. Lett. **90**, 017202 (2003).
[17]The laser energy density cited here does not take into account the possible reflections (about 5%) and absorptions (about 10%) by the lens system used in guiding and collimating the laser beam.
[18]P. Mandal and S. Das, Phys. Rev. B **56**, 15073 (1997).
[19]K. Char, M. S. Colclough, L. P. Lee, and G. Zaharchuk, Appl. Phys. Lett. **59**, 2177 (1991).
[20]S. F. Chen, W. J. Chang, S. J. Liu, J. Y. Juang, J.-Y. Lin, K. H. Wu, T. M. Uen, and Y. S. Gou, Physica B **336**, 267 (2003).
[21]A. M. Haghiri-Gosnet, J. Wolfman, B. Mercey, C. Simon, P. Lecoeur, M. Korzenski, R. Desfeux, and G. Baldinozzi, J. Appl. Phys. **88**, 4257 (2000).
[22]T. Yanagida, T. Kanki, B. Vilquin, H. Tanaka, and T. Kawai, Solid State Commun. **129**, 785 (2004).
[23]B. C. Hauback, H. Fjellvag, and N. Sakai, J. Solid State Chem. **124**, 43 (1996).
[24]G. J. Chen, Y. H. Chang, and H. W. Hsu, J. Magn. Magn. Mater. **219**, 317 (2000).
[25]S. W. Han *et al.*, Phys. Rev. B **69**, 104406 (2004).
[26]J. Y. Lin. W. J. Chang, J. Y. Juang, T. M. Wen, K. H. Wu, Y. S. Gou, J. M. Lee, and J. M. Chen, J. Magn. Magn. Mater. (to be published).